

Published in final edited form as:

*J Infect Dis.* 2009 February 1; 199(3): 445–450. doi:10.1086/596048.

## High Deformability of *Plasmodium vivax*-Infected Red Blood Cells under Microfluidic Conditions

Sarwo Handayani<sup>1</sup>, Daniel T. Chiu<sup>9</sup>, Emiliana Tjitra<sup>1</sup>, Jason S. Kuo<sup>9</sup>, Daniel Lampah<sup>1,2</sup>, Enny Kenangalem<sup>1,2</sup>, Laurent Renia<sup>3</sup>, Georges Snounou<sup>4,5,6</sup>, Ric N. Price<sup>7,8</sup>, Nicholas M. Anstey<sup>8</sup>, and Bruce Russell<sup>3,8</sup>

<sup>1</sup>National Institute of Health Research and Development, Ministry of Health, Jakarta

<sup>2</sup>Menzies School of Health Research–National Institute of Health Research and Development Research Program and District Ministry of Health, Timika, Papua, Indonesia

<sup>3</sup>Laboratory of Malaria Immunobiology, Singapore Immunology Network, Biopolis, Agency for Science Technology and Research (A\*STAR)

<sup>4</sup>Laboratory of Molecular and Cellular Parasitology, Department of Microbiology, Faculty of Medicine, National University of Singapore, Singapore

<sup>5</sup>INSERM Unité 511, Département de Parasitologie, Hôpital Pitié-Salpêtrière

<sup>6</sup>Université Pierre et Marie Curie, Paris, France

<sup>7</sup>Centre for Tropical Medicine, Nuffield Department of Clinical Medicine, University of Oxford, Centre for Clinical Vaccinology and Tropical Medicine, Oxford, United Kingdom

<sup>8</sup>International Health Division, Menzies School of Health Research and Charles Darwin University, Darwin, Australia

<sup>9</sup>Department of Chemistry, University of Washington, Seattle

### Abstract

Maturation of *Plasmodium falciparum* decreases the deformability of infected red blood cells (RBCs), increasing their clearance as they attempt to pass through endothelial slits of the splenic sinus. Previous studies of *Plasmodium vivax*-infected RBCs led to opposite conclusions with respect to cellular deformability. To resolve this controversy, *P. vivax*-infected RBCs were passed through a 2- $\mu$ m microfluidic channel. In contrast to *P. falciparum*-infected RBCs, mature *P. vivax*-infected RBCs readily became deformed through 2- $\mu$ m constrictions. After this extreme deformation, 67% of *P. vivax*-infected RBCs, recovered a normal appearance; however, 15% of uninfected RBCs were destroyed. Results suggest mechanisms for both avoidance of splenic clearance and anemia in vivax malaria.

© 2008 by the Infectious Diseases Society of America. All rights reserved.

Reprints or correspondence: Dr. Bruce Russell, Laboratory of Malaria Immunology, Singapore Immunology Network, 8A Biomedical Grove, #03-06 Immunos, Singapore 138648 (bruce\_russell@immunol.a-star.edu.au).

B.R. conceived and designed the experiments. S.H. and B.R. performed the experiments. S.H. and B.R. analyzed the data. D.T.C., E.T., J.S.K., D.L., E.K., G.S., L.R., R.N.P., and N.M.A. contributed reagents, materials, and analysis tools. G.S., S.H., D.T.C., E.T., J.S.K., L.R., R.N.P., N.M.A., and B.R. wrote the article.

Conflicts of interest: none reported.

The spleen plays a crucial role in removing old, abnormal, and rigid red blood cells (RBCs) that are unable to pass through the  $\sim 2\text{-}\mu\text{m}$  slits between the endothelial cells of the splenic sinusoids. Likewise, parasitized erythrocytes containing bulky viscous *Plasmodium* parasites either are retained by the splenic red pulp or lose their parasites by pitting [1]. Human RBCs infected with *Plasmodium falciparum* have been shown to become increasingly more rigid as the parasite matures, in association with modifications of the infected RBC surface by a range of parasite-derived proteins [2]. It has been postulated that the capacity of maturing *P. falciparum*-infected RBCs to cytoadhere to the endothelium of the vasculature of internal organs has evolved as a means to avoid splenic clearance of these rigid cells [2].

Cytoadherence of parasitized cells and impaired RBC deformability are thought to be the 2 central processes underlying microvascular obstruction and pathology in severe cases of falciparum malaria. Increased rigidity of infected RBCs has been observed for other *Plasmodium* species, such as *P. knowlesi* [3, 4], which can also sequester in the deep vasculature.

The other major but neglected *Plasmodium* species that causes infection in humans is *P. vivax*. Contrary to previous dogma, it is now recognized that *P. vivax* is a major cause of morbidity and mortality [5]. The mechanisms of severe disease and parasite survival in humans with vivax malaria are not known. *P. vivax* displays only a slight tendency to sequester [6], and studies examining the potential role of rheologic changes in parasite survival and clinical disease have shown conflicting results. In an ex vivo flow-based study, Suwanarusk et al. [7] concluded that the deformability increased dramatically, because *P. vivax* trophozoites develop into schizonts. However, ex vivo aggregation and deformability studies suggested a reduction in the deformability of *P. vivax*-infected RBCs [8]. In an effort to resolve this controversy, we report the real-time behavior of single *P. vivax*-infected RBCs in a microfluidic model [9] that presents the infected RBC with a constriction that mimics the splenic filter and the fine capillary beds. Unlike a rheoscope, which deforms erythrocytes purely by shear stress, our constriction-based model subjects erythrocytes to a true extrusion that incorporates multiple mechanical responses, including those resulting from (1) the transient pressure differential experienced by a cell as it travels between the entrance and exit of the constriction, (2) elastic conformation of the cell membrane to rigid external boundaries, and (3) an increase in capillary pressure as a result of membrane curvature change.

## Materials and methods

Eight *P. vivax* and 3 *P. falciparum* isolates were collected from patients attending Rumah Sakit Mitra Masyarakat Hospital in southern Papua Province, Indonesia. Patients with symptomatic malaria were recruited into the study if they were singly parasitized with *P. vivax* or *P. falciparum*, with parasitemia of at least 0.5%. Patients treated with antimalarial agents in the 3 weeks before isolate collection and processing were excluded. The *P. falciparum* isolates were used only if mature trophozoites and schizonts were present in the peripheral blood; consequently, all isolates used were obtained from patients with hyperparasitemia of  $>10\%$ . The median parasitemia of the *P. vivax* isolates used was 0.7% (range, 0.3%–0.8%), with at least 60% of the parasites in the late trophozoite stage; *P. vivax*

schizonts were present in all of isolates. Venous blood was collected into lithium heparin tubes. After removal of >90% of the white blood cells of the host by use of a CF11 column, packed, infected RBCs were washed in PBS and prepared to a hematocrit of 2% in McCoy media (Gibco) supplemented with 20% human serum (buffered pH, 7.2–7.4). Giemsa-stained thick and thin isolates were examined by light microscopy to assess the species and stage of parasites. Two polymerase chain reaction methods were subsequently used to confirm the *Plasmodium* species diagnosis [10].

Poly(dimethylsiloxane) (PDMS) microchannels were constructed using a rapid prototyping method, as described elsewhere [9, 11]. The test samples were mounted onto a Nikon Eclipse TS100 inverted microscope with Nikon 100× and 60× objectives for bright-field and phase contrast imaging, respectively. A one-half-inch monochrome analog CCD camera (Adirondack Astronomy) was used to capture high-speed phase-contrast images for velocity and recovery measurements. Bright-field images were captured using a digital color CCD camera (QImaging). The images then were analyzed frame by frame with the use of QCapture Pro software (version 5.0; QImaging).

Details on the flow control system for samples injected into the microchamber have been presented elsewhere by Shelby et al. [9]. The temperature of the sample above the objective was 32°C (which is the ambient temperature in Papua Province, Indonesia). For each experiment, the velocity of uninfected RBCs in the 25- $\mu\text{m}$  main channel located upstream of the constriction was in the range of 30–50  $\mu\text{m/s}$ , whereas velocities in the 2- $\mu\text{m}$  constriction were as high as 625  $\mu\text{m/s}$ , resulting in a decrease in pressure across this gap of  $\sim 0.4$  mmHg (1 mmHg = 133 Pa) [9] (figure 1A).

The duration of each experiment was no longer than 1 h. Testing of infected RBCs was completed within 2 h after their removal from the patient. The transit time was the time (expressed in seconds) that it took for a RBC to pass through the 2- $\mu\text{m}$  constriction. The recovery time was the time (expressed in seconds) for a deformed RBC exiting the constriction to recover its original shape (figure 2A). Because the median transit and recovery times of uninfected RBCs differed between patients, the median transit and recovery times of infected RBCs from each patient were normalized to the paired uninfected RBC data for each patient.

Data were analyzed using SPSS for Windows (version 15; SPSS). The Mann-Whitney *U* test or the Kruskal-Wallis test was used for nonparametric comparisons, and Student's *t* test (paired and unpaired) or 1-way analysis of variance was used for parametric comparisons of  $\log_{10}$ -transformed data. For categorical variables, percentages and corresponding 95% confidence intervals (95% CIs) were calculated using Wilson's method. Proportions were examined using the  $\chi^2$  test with Yates' correction or Fisher's exact test.

Ethics approval for the present study was obtained from the ethics committees of the National Institute of Health Research and Development, Ministry of Health (Jakarta, Indonesia), and the Menzies School of Health Research, Charles Darwin University (Darwin, Australia).

## Results and discussion

In previous studies, a reduction in the ability of mature stages of *P. falciparum*-infected RBCs to pass through increasingly smaller microfluidic constrictions (8, 6, 4, and 2  $\mu\text{m}$ ) was observed [9, 12]. This reduced movement of *P. falciparum* trophozoites and schizonts through these chambers most likely was the result of increases in both the internal viscosity of infected RBCs and membrane rigidity. These studies were conducted using cloned lines of *P. falciparum* that had been maintained in culture for extended periods. In the present study, we sought to subject parasite material freshly obtained from infected patients to microchambers similar to those used previously.

When fresh, ex vivo clinical isolates of *P. falciparum* ( $n = 3$ ) were subjected to analysis, the infected RBCs were observed to adhere rapidly to the PDMS channel upstream of the constriction. Thus, within 1 min of the addition of the fresh *P. falciparum*-infected RBCs into the chamber, rosettes, uninfected RBC plaques, and agglutinating infected RBCs were formed, and the main channel became occluded, with near total reduction in the flow of both infected RBCs and uninfected RBCs (figure 1B). Consequently, the behavior of individual *P. falciparum*-infected RBCs collected directly from patients could not be assessed in the 2- $\mu\text{m}$  constriction of the microfluidic channels. These observations suggested that fresh clinical isolates of *P. falciparum*-infected RBCs could be far more “sticky” than those derived from laboratory clones. At present, the reasons for this possibility remain a matter for speculation.

In contrast to *P. falciparum*-infected RBCs, *P. vivax*-infected RBCs of all developmental stages were observed to transverse the 2- $\mu\text{m}$  constriction readily. The median transit velocities through this gap decreased with parasite maturity (figure 1C–E), although this was not significant after normalization for variations in the deformability of the uninfected RBCs of the patients (figure 2B). It could be concluded that the increase in the internal viscosity of the infected RBC resulting from the presence of *P. vivax* was offset by the increased deformability of that infected RBC [7]. Interestingly, the size of *P. vivax*-infected RBCs in solution was similar to that of uninfected RBCs ( $\sim 8 \mu\text{m}$ ), which contrasts with the characteristic enlargement of *P. vivax*-infected RBCs observed in thin blood smear specimens (figure 1C–E). Relative to RBCs infected with the less deformable *P. falciparum*, RBCs infected with *P. vivax* tend to spread out, because they are compressed and smeared on the surface of the glass, resulting in the artificially larger surface area observed in *P. vivax* thin films.

Past studies clearly demonstrated that the increased membrane rigidity and internal viscosity of mature parasites further reduce the ability of *P. falciparum*-infected RBCs to recover their shape after constriction [13]. Indeed, *P. falciparum* trophozoites forced through a 4- $\mu\text{m}$  gap took  $\sim 30$  s to recover, whereas schizonts could not do so even after 2 min of observation [9]. The situation was shown to be very different for the highly deformable *P. vivax*-infected RBCs, with 36 (67%) of 54 of the trophozoites and schizonts recovering in a median time of 2.3 s (interquartile range [IQR], 1.2–5.0 s) after traversing a 2- $\mu\text{m}$  gap. The normalized recovery time of infected RBCs was not significantly associated with the developmental stage of the parasite (figure 2C). Despite the high deformability of *P. vivax*-

infected RBCs, the destruction of 18 (33%) of 54 infected cells that passed through the constriction (figure 2C and 2D) denoted increased fragility. This fragility was most pronounced for infected RBCs that contained mature parasites, with only 10 (48%) of 21 and 9 (64%) of 14 of RBCs containing trophozoites and schizonts, respectively, surviving the constriction (figure 2D). The percentage of ring-stage parasites (90% [17 of 19 ring-stage parasites]) surviving passage through the 2- $\mu$ m channel was not significantly different from that observed for the uninfected RBCs (85% [28 of 33 ring-stage parasites];  $P = .638$ ) (figure 2D). Of note, only 2 (3%) of 67 uninfected RBCs collected from a healthy control individual residing in a country of nonendemicity failed to recover when subjected to the same conditions. Because of ethical constraints, we were unable to collect uninfected RBCs from healthy Papuan control subjects.

Our observations offer a number of insights into the pathogenesis of malaria. They demonstrate that *P. vivax*-infected RBCs are highly deformable, confirming previous conclusions derived from flow-based studies [7]. The direct observation of individual cells clearly indicates that microfluidic chambers provide a more realistic measurement than does indirect measurement of infected RBCs [8]. Indeed, microfluidic analysis provides an opportunity to reassess previous conclusions regarding the rigidity of RBCs infected by other parasite species. The sharp contrast between the behavior of RBCs infected with *P. vivax* and that of rigid RBCs infected with *P. falciparum*, the other major parasite species that infects humans, provides a plausible explanation as to how *P. vivax* avoids splenic clearance despite the inability of its mature stages to sequester significantly. An additional consequence of the lack of rigidity of *P. vivax*-infected RBCs is a decreased likelihood that these cells block capillary beds in internal organs, thus reducing the frequency of severe organ-specific clinical manifestations, compared with the frequency noted in association with *P. falciparum* infections.

Alternative explanations are needed for the severe manifestations that are seen in association with *P. vivax* malaria, particularly severe anemia [5]. A substantial proportion (15%) of uninfected RBCs from patients infected with *P. vivax* failed to recover passage through the splenic sinusoid-like 2- $\mu$ m channel. This substantial ex vivo destruction of uninfected RBCs in vivax malaria supports in vivo findings of a level of anemia that is considerably greater than that attributable to destruction of infected RBCs found in human volunteers experimentally infected with *P. vivax* [14], compared with those infected with *P. falciparum* [14, 15]. The mechanism by which *P. vivax* infections might damage uninfected RBCs is unknown, although either oxidative stress resulting from rupturing parasites or host immune mechanisms have been suggested [16]. Finally, the unexpected contrast between the observations previously made with regard to in vitro-cultured *P. falciparum*-infected RBCs and the observations made in the present study regarding the freshly isolated parasites further reinforces the usefulness of deploying microfluidic devices in a clinical setting, because the data collected may better reflect the phenotypes of infected RBCs relevant to the pathogenesis of malaria infection.

## Acknowledgments

We thank Paulus Sugiarto and the staff of Rumah Sakit Mitra Masyarakat Hospital. We also thank Ferryanto Chalfein, for his expert technical assistance in the field; Rossarin Suwanarusk, for polymerase chain reaction confirmation of the *Plasmodium* species; and solar physicist Alan Brockman, for the use of his CCD camera.

Financial support: Wellcome Trust–National Health and Medical Research Council (NHRMC; Wellcome Trust ICRG GR071614MA–NHRMC ICRG ID 283321 [for funding of the study site]); NHRMC Howard Florey Fellowship (to B.R.); Wellcome Trust–Mahidol University–Oxford Tropical Medicine Research Programme (Wellcome Trust Career Development award 074637 [to R.P.]); NHRMC Practitioner Fellowship (to N.A.); Puget Sound Partners for Global Health (for support of a pilot project by D.T.C).

## References

1. Angus BJ, Chotivanich K, Udomsangpetch R, White NJ. In vivo removal of malaria parasites from red blood cells without their destruction in acute falciparum malaria. *Blood*. 1997; 90:2037–40. [PubMed: 9292540]
2. Cooke BM, Mohandas N, Coppel RL. The malaria-infected red blood cell: structural and functional changes. *Adv Parasitol*. 2001; 50:1–86. [PubMed: 11757330]
3. Miller LH, Usami S, Chien S. Alteration in the rheologic properties of *Plasmodium knowlesi*-infected red cells: a possible mechanism for capillary obstruction. *J Clin Invest*. 1971; 50:1451–5. [PubMed: 4996884]
4. Miller LH, Fremount HN, Luse SA. Deep vascular schizogony of *Plasmodium knowlesi* in *Macaca mulatta*: distribution in organs and ultrastructure of parasitized red cells. *Am J Trop Med Hyg*. 1971; 20:816–24. [PubMed: 5002246]
5. Price RN, Tjitra E, Guerra CA, Yeung S, White NJ, Anstey NM. Vivax malaria: neglected and not benign. *Am J Trop Med Hyg*. 2007; 77:79–87. [PubMed: 18165478]
6. Garnnham, PCC. Malaria parasites and other haemosporidia. Blackwell Scientific Publications; Oxford: 1966.
7. Suwanarusk R, Cooke BM, Dondorp AM, et al. The deformability of red blood cells parasitized by *Plasmodium falciparum* and *P. vivax*. *J Infect Dis*. 2004; 189:190–4. [PubMed: 14722882]
8. Jayavanth S, Jagadeesan K, Singh M. Influence of *P. vivax* malaria on erythrocyte aggregation and deformability. *Clin Hemorheol Microcirc*. 2004; 31:257–66. [PubMed: 15567895]
9. Shelby JP, White J, Ganesan K, Rathod PK, Chiu DT. A microfluidic model for single-cell capillary obstruction by *Plasmodium falciparum*-infected erythrocytes. *Proc Natl Acad Sci USA*. 2003; 100:14618–22. [PubMed: 14638939]
10. Boonma P, Christensen PR, Suwanarusk R, Price RN, Russell B, Lek-Uthai U. Comparison of three molecular methods for the detection and speciation of *Plasmodium vivax* and *Plasmodium falciparum*. *Malar J*. 2007; 6:124. [PubMed: 17868467]
11. McDonald JC, Duffy DC, Anderson JR, et al. Fabrication of microfluidic systems in poly(dimethylsiloxane). *Electrophoresis*. 2000; 21:27–40. [PubMed: 10634468]
12. Antia M, Herricks T, Rathod PK. Microfluidic modeling of cell-cell interactions in malaria pathogenesis. *PLoS Pathog*. 2007; 3:e99. [PubMed: 17658948]
13. Cranston HA, Boylan CW, Carroll GL, et al. *Plasmodium falciparum* maturation abolishes physiologic red cell deformability. *Science*. 1984; 223:400–3. [PubMed: 6362007]
14. Collins WE, Jeffery GM, Roberts JM. A retrospective examination of anemia during infection of humans with *Plasmodium vivax*. *Am J Trop Med Hyg*. 2003; 68:410–2. [PubMed: 12875288]
15. Dondorp AM, Angus BJ, Chotivanich K, et al. Red blood cell deformability as a predictor of anemia in severe falciparum malaria. *Am J Trop Med Hyg*. 1999; 60:733–7. [PubMed: 10344643]
16. Dondorp AM, Pongponratn E, White NJ. Reduced microcirculatory flow in severe falciparum malaria: pathophysiology and electron-microscopic pathology. *Acta Trop*. 2004; 89:309–17. [PubMed: 14744557]

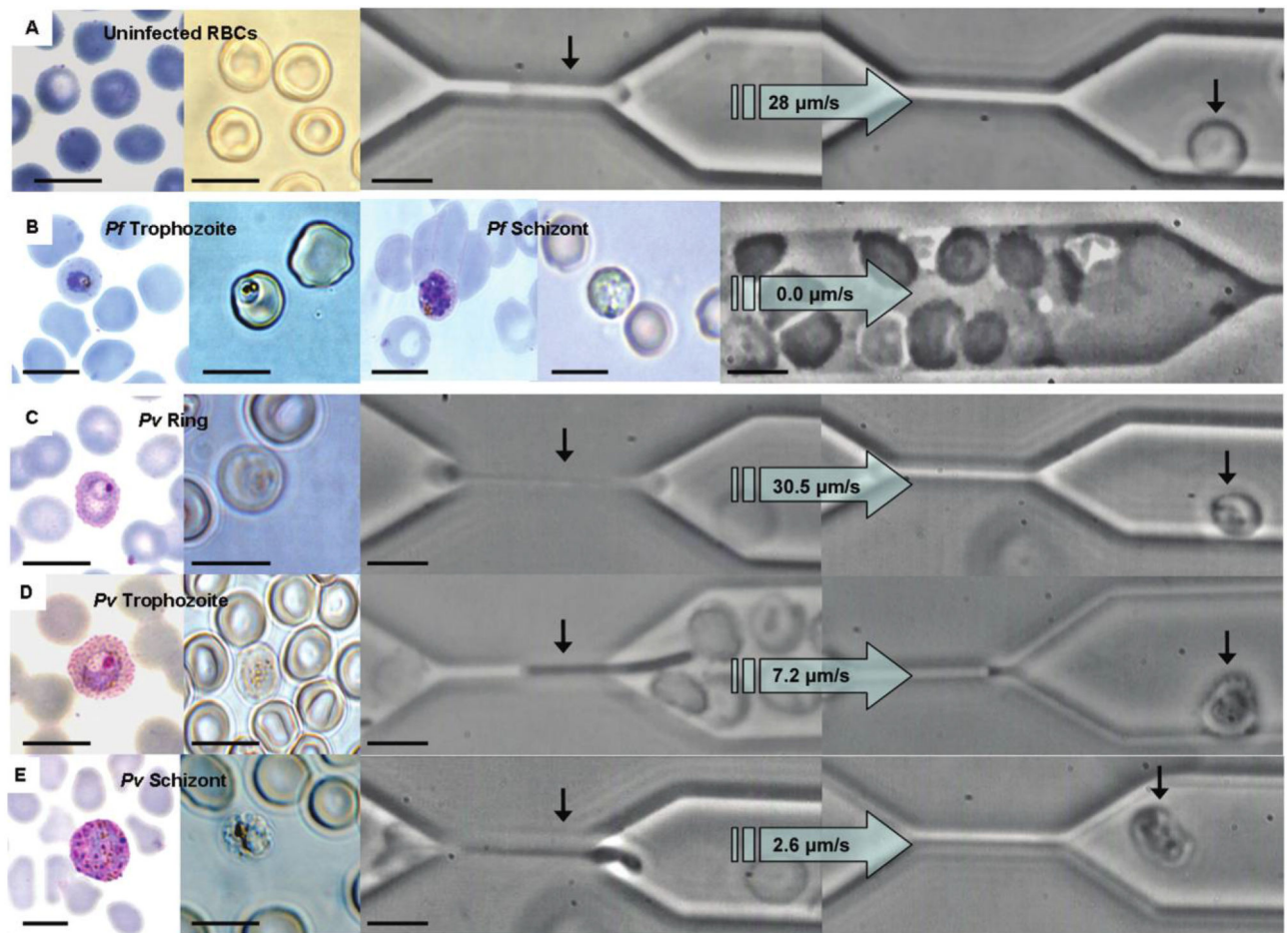


**Figure 1.**

Transit of uninfected red blood cells (RBCs) or *Plasmodium falciparum*- and *Plasmodium vivax*-infected RBCs through the 2- $\mu$ m constriction of the microfluidic chamber. On the left side of each panel, the representative cell stage is shown either stained with Giemsa (fixed) or unstained (fresh) under bright-field illumination. On the right side of each panel is a phase-contrast image of cells as they transit through the 2- $\mu$ m constriction. **A**, Uninfected RBCs from vivax malaria isolates moved through the channel with a median velocity of 28.0  $\mu$ m/s (range, 9.9–625  $\mu$ m/s). **B**, The microfluidic channel was blocked within 60 s of the addition of clinical isolates of *P. falciparum* trophozoites and schizonts. **C–E**, The median velocity of *P. vivax* rings, trophozoites, and schizonts was 30.5  $\mu$ m/s (range, 1.9–354  $\mu$ m/s), 7.2  $\mu$ m/s (range, 0.7–34.9  $\mu$ m/s), and 2.6  $\mu$ m/s (range, 0.8–11.7  $\mu$ m/s), respectively. Note the increased size of *P. vivax*-infected RBCs relative to uninfected RBCs and *P. falciparum*-infected RBCs in the Giemsa-stained smears, despite the infected RBCs of both species having a similar diameter in the fresh preparation. The horizontal black scale bars denote 10  $\mu$ m. The large arrows denote the direction of flow and velocity of the RBC moving through the constriction. *Pf*, *P. falciparum*; *Pv*, *P. vivax*.

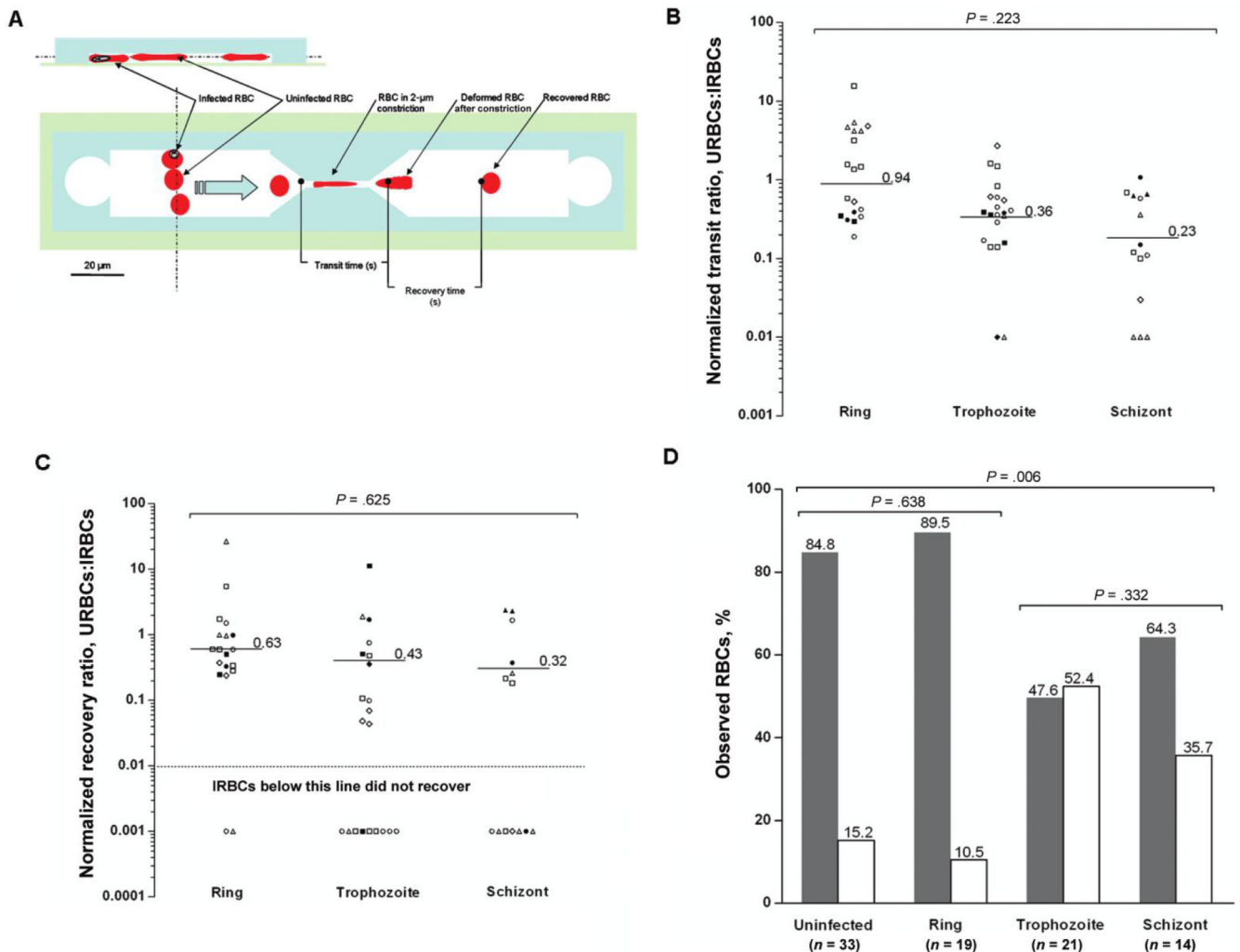


**Figure 2.**

The effect of asexual development of *Plasmodium vivax* on recovery or destruction of infected red blood cells (IRBCs) after passage through the 2- $\mu$ m constriction. **A**, Side and plan scale view diagrams of the poly(dimethylsiloxane) (PDMS) microfluidic channel used to model splenic clearance of IRBCs. See Materials and Methods for definitions of transit and recovery times. The blue arrow denotes the direction of flow. The light green-shaded area represents the borosilicate glass coverslip attached to the PDMS (light blue-shaded area) chamber. **B**, The normalized transit ratio of the *P. vivax* ring, trophozoite, and schizont stages moving through the 2- $\mu$ m constriction. The transit ratio was calculated by normalizing the velocity of each of the IRBCs against the median transit velocity of uninfected RBCs (URBCs) from the same isolate. The 8 different symbols each denote an isolate. The horizontal lines denote the median of the median isolate transit ratio for each developmental stage. The arrow on the y-axis indicates that the transit ratio is proportional to the cell velocity. The transit ratio did not significantly decrease as the parasite developed from ring to schizont stage ( $P = .223$ ; 8 isolates and 87 cells). **C**, The recovery ratio for IRBCs was calculated by normalizing the time to recovery of each of the IRBCs against the



median time to recovery of URBCs from the same isolate. The 8 different symbols each denote an isolate. The horizontal lines denote the median of the median isolate recovery ratio for each developmental stage. The arrow on the axis indicates that the recovery ratio is proportional to the rate of recovery of cell shape. The recovery ratio was not significantly effected by the stage of parasite development ( $P = .625$ ; 8 isolates and 54 cells). Data from IRBCs and URBCs destroyed by constriction were not included in the median recovery times (18 cells are shown under the red dashed lines). *D*, Although there was no significant difference between the percentage of URBCs and ring-stage IRBCs destroyed ( $P = .638$ ), a significantly higher percentage of trophozoite- and schizont-infected red blood cells (RBCs) were destroyed by the constriction ( $P = .006$ ). Shaded bars denote the percentage of RBCs not destroyed by the constriction. Unshaded bars denote the percentage of RBCs destroyed by the constriction.